Tsix–Mecp2 female mouse model for Rett syndrome reveals that low-level MECP2 expression extends life and improves neuromotor function

Lieselot L. G. Carrette[a,b,c,d], Roy Blum[a,b,c], Weiyuan Ma[e,f], Raymond J. Kelleher III[e,f], and Jeannie T. Lee[a,b,c,1]

[a]Howard Hughes Medical Institute, Massachusetts General Hospital, Boston, MA 02114; [b]Department of Molecular Biology, Massachusetts General Hospital, Boston, MA 02114; [c]Department of Genetics, Harvard Medical School, Boston, MA 02115; [d]Center for Medical Genetics, Ghent University, 9000 Ghent, Belgium; [e]Center for Genomic Medicine, Massachusetts General Hospital, Boston, MA 02114; and [f]Department of Neurology, Massachusetts General Hospital, Boston, MA 02114

Contributed by Jeannie T. Lee, June 20, 2018 (sent for review January 17, 2018; reviewed by Michela Fagiolini and Monica J. Justice)

Rett syndrome (RTT) is a severe neurodevelopmental disorder caused by a mutation in the X-linked methyl-CpG-binding protein 2 (MECP2). There is currently no disease-specific treatment, but MECP2 restoration through reactivation of the inactive X (Xi) has been of considerable interest. Progress toward an Xi-reactivation therapy has been hampered by a lack of suitable female mouse models. Because of cellular mosaicism due to random X-chromosome inactivation (XCI), *Mecp2*$^{+/-}$ heterozygous females develop only mild RTT. Here, we create an improved female mouse model by introducing a mutation in *Tsix*, the antisense regulator of XCI allelic choice. *Tsix–Mecp2* mice show reduced MECP2 mosaicism and closely phenocopy the severely affected *Mecp2*-null males. *Tsix–Mecp2* females demonstrate shortened lifespan, motor weakness, tremors, and gait disturbance. Intriguingly, they also exhibit repetitive behaviors, as is often seen in human RTT, including excessive grooming and biting that result in self-injury. With a *Tsix* allelic series, we vary MECP2 levels in brain and demonstrate a direct, but nonlinear correlation between MECP2 levels and phenotypic improvement. As little as 5–10% MECP2 restoration improves neuromotor function and extends lifespan five- to eightfold. Our study thus guides future pharmacological strategies and suggests that partial MECP2 restoration could have disproportionate therapeutic benefit.

Rett syndrome | MECP2 | X reactivation | Tsix | Xist

Rett syndrome (RTT) is a human neurodevelopmental disorder caused by a mutation in methyl-CpG-binding protein 2 (MECP2) (1, 2), a chromatin-associated gene product that is crucial for neuronal development. The disease typically occurs sporadically and most commonly arises from a de novo mutation in the paternal germline (3). RTT thus appears most frequently in girls and affects 1 in 10,000 newborn girls (2, 4, 5). In rare cases, RTT manifests in boys who can inherit the mutation from their unaffected mothers, but typically succumb to the disorder within the first year (6). On the other hand, newborn girls initially develop normally, but begin to lose learned abilities later in the first year, with progression to full-blown disease in subsequent years. After missing developmental milestones, the girls develop a loss of mobility, severe seizures, breathing abnormalities, and social withdrawal. Patients have absent speech, lose purposeful hand movements, and engage in stereotypic hand wringing and biting. Such repetitive behaviors are often self-injurious and can add significantly to morbidity. Indeed, RTT is one of the most severely debilitating genetic illnesses and patients generally require around-the-clock care. A sudden and untimely death is common, although recent improvements in healthcare are helping to extend lifespan. Nonetheless, there is presently no disease-specific treatment or cure, as all available therapies address symptoms rather than the underlying cause. Thus, RTT is a disorder of serious unmet need.

Remarkably, studies in mice have shown that restoring expression of MECP2 protein to the brain after disease onset can reverse the disorder (7, 8). These promising findings have led to efforts to restore MECP2 expression to patients with RTT (5). An advantage of such an approach is correction of the underlying defect—absence of MECP2—rather than merely treating symptoms. Therapeutic strategies for MECP2 restoration have centered on two approaches: (*i*) gene therapy that delivers exogenous *MECP2* minigenes via AAV vectors to the brain, and (*ii*) reactivation of the dormant copy of *MECP2* that is carried on the inactive X chromosome (Xi) using small molecule drugs or biologics. Xi reactivation may be advantageous to gene therapy because of a lower likelihood that MECP2 would be overexpressed. MECP2 overexpression also causes neurological disease (9).

The Xi-reactivation approach is predicated on "X-chromosome inactivation" (XCI), an epigenetic process that silences one of two X chromosomes during early female development to compensate for dosage differences between XX females and XY males (10, 11). XCI renders every female mammal a mosaic of cells that express either the maternal or paternal X chromosome. Heterozygous X-linked mutations therefore affect only half of a female's somatic cells, on average. Significantly, in affected cells, a normal copy of *MECP2* lies dormant on the Xi. Efforts to reactivate the silent allele of *MECP2* have shown increasing promise in recent years (12–17). Included among these efforts is our recent study

Significance

Rett syndrome (RTT) is an X-linked neurodevelopmental disorder caused by mutations in *MECP2*. To treat RTT, reactivating the dormant copy of *MECP2* on the inactive X has been of considerable interest. Although potential therapeutics have been identified, their development has been hampered by the lack of a suitable female mouse model and uncertainty regarding how much MECP2 needs to be restored. Here, we create a female model with a more severe phenotype, including a short lifespan, neuromotor impairment, and repetitive behaviors often seen in human RTT. Significantly, 5–10% MECP2 restoration in brain extends lifespan by eightfold and improves RTT phenotypes. Our study thus provides a much-needed female model and implies potential therapeutic benefit with low-level MECP2 expression.

Author contributions: L.L.G.C. and J.T.L. designed research; L.L.G.C. performed research; R.B., W.M., and R.J.K. contributed analytic tools; L.L.G.C. and J.T.L. analyzed data; and L.L.G.C. and J.T.L. wrote the paper.

Reviewers: M.F., Boston Children's Hospital and Harvard Medical School; and M.J.J., The Hospital for Sick Children.

The authors declare no conflict of interest.

[1]To whom correspondence should be addressed. Email: lee@molbio.mgh.harvard.edu.

This article contains supporting information online at www.pnas.org/lookup/suppl/doi:10.1073/pnas.1800931115/-/DCSupplemental.

Published online July 23, 2018.

demonstrating that a mixed-modality approach, which combines a small molecule DNA methylation inhibitor and antisense oligonucleotide (ASO) directed against Xist RNA, can achieve 30,000-fold reactivation of MECP2 from the Xi (16).

An important next step in advancing an Xi-reactivation therapeutic is the development of a suitable mouse model in which Xi-reactivating drugs can be tested. Nearly all RTT research in small animal models presently utilizes male mice (18), as hemizygous animals consistently develop a severe RTT-like disorder characterized by stiff, uncoordinated gait and rapid weight loss at 3 wk (18, 19). RTT males invariably succumb to the disease within the first 3 mo. However, because male mice do not harbor an Xi, they are not appropriate subjects to test Xi-reactivating drugs. Although female mice can be generated from three available RTT alleles (19–21), they make suboptimal subjects because they have a nearly normal lifespan and develop only a mild disease. Although certain phenotypic characteristics such as visual evoked potentials (22), pup retrieval (23), purposeful use of forepaws (24), motor deficits (25), and breathing abnormalities (26) can be used to evaluate female disease, these phenotypes develop only in a subset of *Mecp2*$^{+/-}$ females. Importantly, the random nature of XCI leads to heterogeneous tissue contribution of affected cells, and this cellular mosaicism in turn leads to variable penetrance of the disease. Disease penetrance can also be complicated by strain background (19, 20, 25, 27) and parenting (28). Here, by taking advantage of the XCI machinery, we engineer a female RTT mouse model with reduced cellular mosaicism and full disease penetrance. Using these mice, we discover that low-level MECP2 expression in the brain can have a disproportionately positive impact on health and survival.

Results

XCI is directed by a noncoding master locus known as the X-inactivation center (Xic) that controls various steps of XCI, including chromosome counting, choice, and establishment of silencing (10, 11). The *Xic* produces the long noncoding RNA, Xist (X-inactive specific transcript) (29), which spreads over the future Xi, recruiting silencer proteins, and thereby establishes the inactive state across the X chromosome. *Xist* is, in turn, controlled by another noncoding locus, *Tsix*, which produces the antisense transcript that blocks expression and action of Xist *in cis* (30). In female cells, deleting *Tsix* results in constitutive upregulation of *Xist in cis*. Thus, in addition to controlling *Xist* expression, *Tsix* also controls the choice of which the X chromosome will be inactivated. In the unperturbed state, each X chromosome has an equal chance of being inactivated, but the ratio can be skewed when mutations are introduced into *Tsix*. With this knowledge, we took advantage of existing synthetic knockouts of *Tsix* (*Tsix*$^{\Delta F}$, *Tsix*$^{\Delta CpG}$) (31, 32) and generated a heterozygous mouse deficient for *Tsix* and *Mecp2* on opposite X chromosomes (*Tsix*$^{-/+}$ *Mecp2*$^{+/-}$) (Fig. 1 *A* and *B*), in an effort to create a female mouse in which the null *Mecp2* allele would be preferentially expressed and the wild-type (WT) allele would lie dormant on the Xi.

The *Tsix*$^{\Delta F}$ allele results from a 3.7-kb deletion of *Tsix's* CpG island (32) (Fig. 1*A*). We crossed the *Tsix*$^{\Delta F}$ allele into the *Mecp2*-null mice (19) to create *Tsix*$^{\Delta F/+}$ *Mecp2*$^{+/-}$ heterozygotes (Fig. 1*B*, cross 2) and examined the effect on lifespan (Fig. 1*C*). Indeed, the average survival of *Tsix*$^{\Delta F/+}$ *Mecp2*$^{+/-}$ females—hereafter "ΔF-RTT" females—was 246 d, significantly lower than that of RTT (*Mecp2*$^{+/-}$) females whose life expectancy was typically >>1 y (often normal). Given that the *Tsix*$^{\Delta F}$ allele was expected to lead to extreme skewing to favor expression of the null *Mecp2* allele (31, 32), we were surprised that the ΔF-RTT females still lived much longer than RTT (*Mecp2*$^{-/Y}$) males. The average life expectancy of RTT males was only 68 or 76 d, depending on whether the father was WT (cross 1) or carried the *Tsix*$^{\Delta F}$ allele (cross 2), respectively (Fig. 1*C*). We surmised that a small percentage of MECP2^{+} cells might be positively selected in the brain, thereby ameliorating the RTT phenotype.

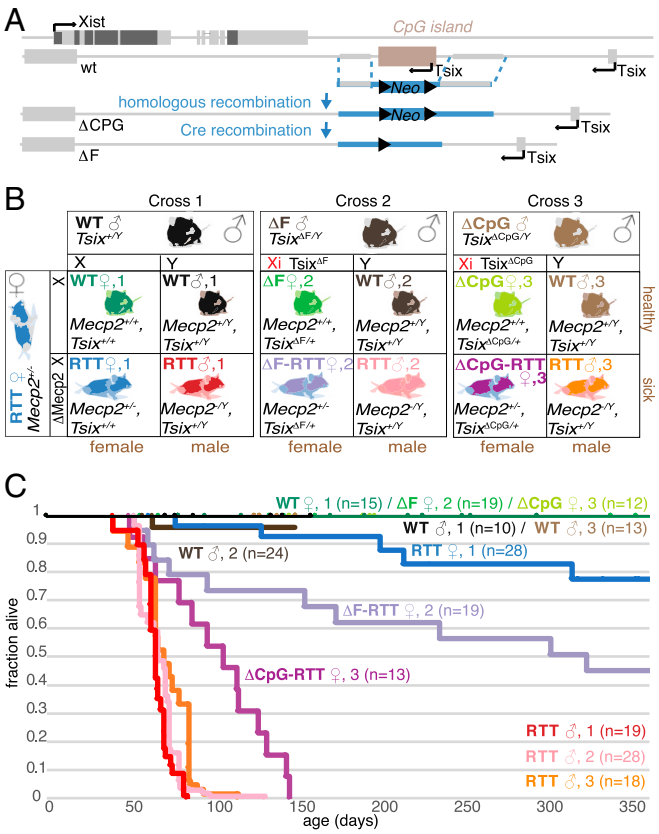

Fig. 1. The *Tsix*$^{-/+}$ *Mecp2*$^{+/-}$ female mouse models increase disease penetrance and reduce disease variability. (*A*) The *Tsix* locus and allelic series. (*B*) Mating scheme to generate the conventional RTT model (cross 1), the ΔF-RTT female model (cross 2), and the ΔCpG-RTT female model (cross 3). Color coding here and throughout the article is as follows: RTT females, blue; RTT males, red; WT females, green; WT males, brown. RTT females [B6.129P2(C)-Mecp2tm1.1Bird/J] were mated with WT (C57BL/6J) or Tsix-deleted (ΔF or ΔCpG) males. The latter were maintained as homozygous lines on a mixed B6/129 background. Thus, the *Tsix*-RTT cross yielded mice of mixed background, which served to improve breeding and overall robustness of the mice (19, 20, 25, 27), with lower frequency of runting even with disease. In all comparisons, littermates from the same cross were analyzed to minimize background effects. (*C*) Kaplan–Maier survival curves for each indicated genotype. Mutants and littermates from crosses 1, 2, and 3 bear the colors of *B*.

To examine whether XCI skewing may be less than expected, we followed ΔF-RTT females across their lifespan and isolated fresh brain tissue from moribund mice. We examined whole brain MECP2 protein levels by Western blot analysis and observed an intriguing variability in the amount of MECP2 protein, with some ΔF-RTT females having no detectable MECP2, whereas others having levels as high as 20% of WT levels (Fig. 2). These levels of MECP expression were rather unexpected, given that the *Tsix* mutation generally skews XCI patterns to an extreme, with only 2.5% of cells typically choosing the WT X chromosome as the active X (31). These data suggest that mutant cells lacking MECP2 protein could indeed be at a selective disadvantage during development, enabling cells that express WT MECP2 to outgrow mutant cells and account for a larger fraction of somatic cells in the adult. Such skewed XCI patterns have been reported in patients with RTT (33).

Next, we investigated the *Tsix*$^{\Delta CpG}$ allele, which has the identical 3.7-kb deletion of *Tsix*, but which still bears the oppositely oriented Neo cassette (31, 34) (Fig. 1*A*). The *Tsix*$^{\Delta CpG}$ allele

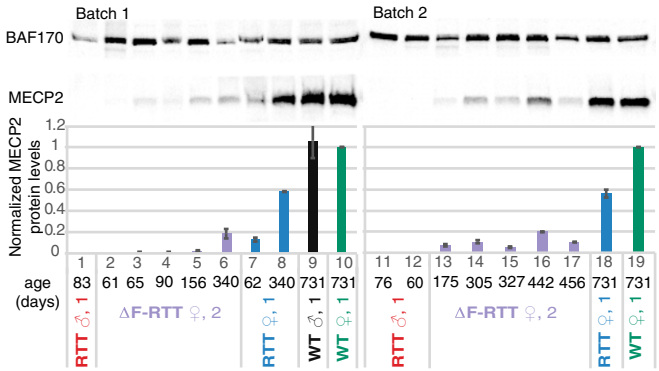

Fig. 2. Variable MECP2 expression in the brain of ΔF-RTT female mice. Western blot analysis of MECP2 protein in whole brain with BAF170 as loading control of different mice (labeled 1–19) of indicated genotypes at the end of life. Lifespan of each mouse is indicated. Error bars represent three technical replicates. Two different batches of ΔF-RTT female mice are shown.

exhibits a stronger skewing phenotype than $Tsix^{\Delta F}$, believed to be due to transcriptional interference caused by the antiparallel orientation of *Neo* transcription (31, 32). We crossed $Tsix^{\Delta CpG/Y}$ males with $Mecp2^{+/-}$ females (19) to obtain $Tsix^{\Delta CpG/+}$ $Mecp2^{+/-}$ female mice—henceforth, "ΔCpG-RTT" females (Fig. 1*B*, cross 3). Western blot analysis of brain tissue from moribund animals suggested undetectable levels of MECP2 relative to WT, consistent with the expected near-complete skewing of XCI ratios to favor expression of the null *Mecp2* allele (Fig. 3*A*). MECP2 levels were similarly low in premorbid mice (*SI Appendix*, Fig. S1). However, in both premorbid and moribund ΔCpG-RTT females, 10- to 20-fold overexposure of the Western blot revealed trace levels of MECP2, indicating levels that were <<5% of WT (*SI Appendix*, Fig. S1).

ΔCpG-RTT females demonstrated severe shortening of lifespan (Fig. 1*C*). The average lifespan of 102 d approximated the truncated life expectancy of the $Mecp2^{-/Y}$ male model. In contrast to RTT and ΔF-RTT females, there was little variability in life expectancy between ΔCpG-RTT females. Immunohistochemistry (IHC) for MECP2 confirmed loss of MECP2 expression in brain regions relevant for RTT (35), including the cortex, hippocampus, and cerebellum, compared with $Tsix^{\Delta CpG/+}$ females with wild-type *Mecp2*, who showed MECP2 staining throughout the brain (Fig. 3*B* and *SI Appendix*, Fig. S2). RTT females without *Tsix* deletion exhibited strong MECP2 staining in about half of the cells, in accordance with cellular mosaicism, while RTT males showed no MECP2 staining at all. On the other hand, the ΔCpG-RTT females showed an occasional but rare $MECP2^+$ cell, in agreement with an extreme but incomplete skewing of XCI. These rare cells did not produce enough MECP2 (<<5% of wild-type levels) to be detectable by Western blotting (Fig. 3*A*), except when overexposed (*SI Appendix*, Fig. S1), but would be consistent with secondary selection for $MECP2^+$ cells in the brain and could also explain why ΔCpG-RTT females live ∼3 wk longer than the fully null RTT males. Occasionally, $MECP2^+$ cells showed regional clustering (Fig. 3*C*). Such clustering could potentially further contribute to the small degree of phenotypic variation between ΔCpG-RTT females. Thus, by skewing XCI ratios to an extreme, we effectively decreased MECP2 mosaicism and increased disease penetrance in the female model.

The *Tsix* allelic series and the resulting variable expression of MECP2 provided an unprecedented opportunity to study the

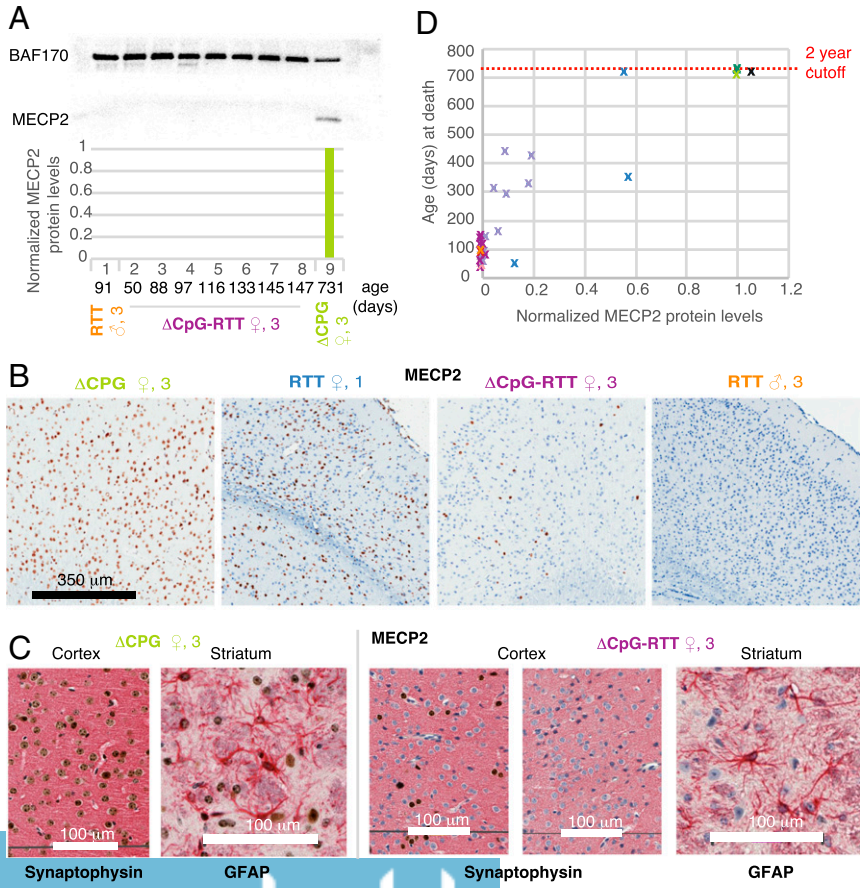

Fig. 3. The ΔCpG-RTT female mouse model shows reduced MECP2 cellular mosaicism and increased disease penetrance. (*A*) Western blot analysis of MECP2 protein in whole brain with BAF170 as loading control of different mice (labeled 1–9) of indicated genotypes at the end of life. Lifespan of each mouse is indicated. Error bars represent three technical replicates. (*B*) MECP2 immunohistochemistry of cortex on fixed brain slices of ΔCpG, RTT, ΔCpG-RTT females, and RTT male. ΔCpG, ΔCpG-RTT females, and RTT male from cross 3 were 2 mo old. RTT female from cross 1 was 1 y old when killed. (*C*) Double IHC staining for MECP2 and synaptophysin (control neuronal marker) of cortical regions and for MECP2 and GFAP (control glial marker) of striatum of ΔCpG and ΔCpG-RTT females from *B*. Note patchy MECP2 expression in ΔCpG-RTT females. (*D*) Correlation between MECP2 protein levels in the brain of moribund mice and lifespan.

relationship between MECP2 levels and severity of RTT phenotypes—and the larger question of how many MECP2^{+} cells in the brain are necessary for phenotypic improvement. We correlated MECP2 protein levels with lifespan and found an intriguing nonlinear positive correlation (Fig. 3*D*). ΔCpG-RTT females (dark purple Xs, Fig. 3*D*) and ΔF-RTT females (light purple Xs) with undetectable MECP2 levels showed a severely shortened lifespan of <100 d. Remarkably, an MECP2 protein level of only 5% doubled the lifespan to 160 d, and protein levels of 10–20% further extended life to 400 d (Fig. 3*D*). Thus, a small increase in MECP2 levels and in the number of MECP2-expressing cells has a disproportionately positive impact on phenotype as measured by life expectancy.

We then asked whether extended life expectancy was accompanied by qualitative improvements in neuromotor function, an important readout for RTT symptoms. We subjected ΔF-RTT and ΔCpG-RTT females to mobility paradigms for RTT that are easy to score objectively. One such paradigm is the rotarod test, which examines forced muscle activity and provides a measure of both motor strength and coordination. We placed 9-wk-old mice on an accelerating rotating beam and recorded the length of time they stay engaged on the beam (36). At 9 wk, several RTT males had already perished, but enough remained healthy enough to be tested. One-way ANOVA indicated a significant difference between the groups in Fig. 4*A* ($P = 3.7 \times 10^{-39}$). As expected, RTT males performed poorly, relative to WT males ($P < 0.001$ for crosses 1–3). RTT females performed essentially equal as WT females ($P = 0.73$). Significantly, ΔCpG-RTT and ΔF-RTT females performed much worse than WT females ($P = 9.8 \times 10^{-13}$ and $P = 5.9 \times 10^{-12}$, respectively) and also relative to RTT females ($P = 0.062$ and $P = 0.0032$, respectively). The general differences were captured not only by the quantitative measurements but also by qualitative distinctions evident in video recordings (Movies S1 and S2).

Another oft-used mobility paradigm is gait analysis, in which paw prints of a mouse that traverses a runway toward a goal box are captured and the distance between the footfalls of the front and back paw measured (Fig. 4*B*) (37). Gait analysis further accentuated the difference between ΔCpG-RTT, ΔF-RTT, and RTT females. Healthy mice demonstrate a characteristic manner of walking in which the front (red) and back (blue) paw prints overlap with each stride (Fig. 4*B*). By contrast, RTT males displayed a severe gait disturbance in which there was clear separation of front and back paw prints (Fig. 4 *B* and *C*). Welch's ANOVA indicated a significant difference between the groups ($P = 1.1 \times 10^{-11}$ for distance and $P = 5.0 \times 10^{-6}$ for number). While RTT females did not show a strong gait phenotype yet at 9 wk ($P = 0.22$ for distance, Fig. 4*C* and $P = 0.98$ for number, *SI Appendix*, Fig. S1), the *Tsix*$^{-/+}$ *Mecp2*$^{+/-}$ females did, with the ΔCpG-RTT females demonstrating a much stronger phenotype than the ΔF-RTT in terms of both stride length and number of steps bigger than a chosen threshold value (ΔF-RTT: $P = 5.5 \times 10^{-5}$ for distance and $P = 0.010$ for number. ΔCpG-RTT: $P = 7.9 \times 10^{-4}$ for distance and $P = 0.054$ for number) (Movie S3). The gait disturbance was also evident from shorter stride lengths, with resulting greater number of steps required to complete the traversal, a more outward placement of back and inward placement of front paws, presumptively for increased stability due to muscle weakness, rendering the tracks more like bunny hops. Overall, ΔCpG-RTT females more closely phenocopied RTT male littermates on all neuromotor tests.

As the ΔCpG-RTT stood out among female RTT models, we investigated other aspects of the disease. Body mass in RTT has been reported to be variable in some female mouse models, but consistently drops rapidly in male models, especially at the end stage (Fig. 5*A*). In ΔCpG-RTT females, a large weight variation was observed compared with WT females, potentially due to disease-induced weight fluctuations at various disease stages for ΔCpG-RTT females (Fig. 5*B*). The variance was nonhomogeneous between WT and ΔCpG-RTT females as calculated by Levene's test at 9, 13, and 17 wk ($P = 0.001$, 0.009, and 0.003, respectively). Neurological symptoms also became evident over the course of the shortened lifespan. In the conventional RTT females, visible neurological symptoms such as hindlimb clasping, tremors, and gait abnormalities first appeared around 6 mo of age. At 17 wk, only 10% showed symptoms (19). By contrast, the ΔCpG-RTT females showed early onset of symptoms, appearing from weaning age (3–4 wk) onwards and phenocopying the RTT males, albeit with slightly slower progression of the disease (Fig. 5*C*). For ΔCpG-RTT females, a strong tremor was one of the first and clearest symptoms noticeable upon weaning (Movie S4). ΔCpG-RTT females also developed reduced movement, abnormal gait, and a later onset of hindlimb clasping (Movies S4–S9). The presentation therefore differed significantly from that of RTT females, for whom hindlimb

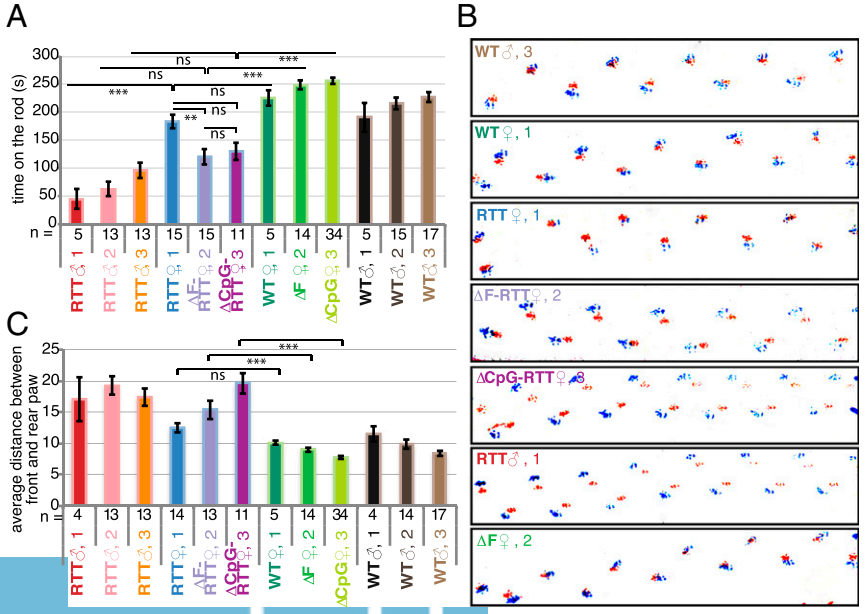

Fig. 4. Mobility tests for neuromotor function. (*A*) Summary of the rotarod analysis showing the average time on the rod in seconds for 9-wk-old mice of the indicated control and test genotypes. Sample size (*n*) is shown below each bar. ANOVA, $P = 3.7 \times 10^{-39}$. *P* values in pairwise comparisons calculated using Tukey's honest significance test (ns, nonsignificant, $^{**}P < 0.01$ and $^{***}P < 0.001$ for the indicated comparisons). Error bars represent the SE on mean (SEM). (*B*) Representative pawprint tracks during gait analysis of each indicated test and control genotype. Mice were tested at 9 wk of age. Front paws, red; rear paws, blue. (*C*) Plot of gait analysis, showing the average distances between front and rear paws of experiments in *B*. Sample sizes (*n*) are shown below each bar. Welch's ANOVA, $P = 1.1 \times 10^{-11}$. *P* values in pairwise comparisons were calculated using the Games–Howell post hoc test (ns, nonsignificant, $^{***}P < 0.001$ for the indicated comparisons). Error bars represent SEM.

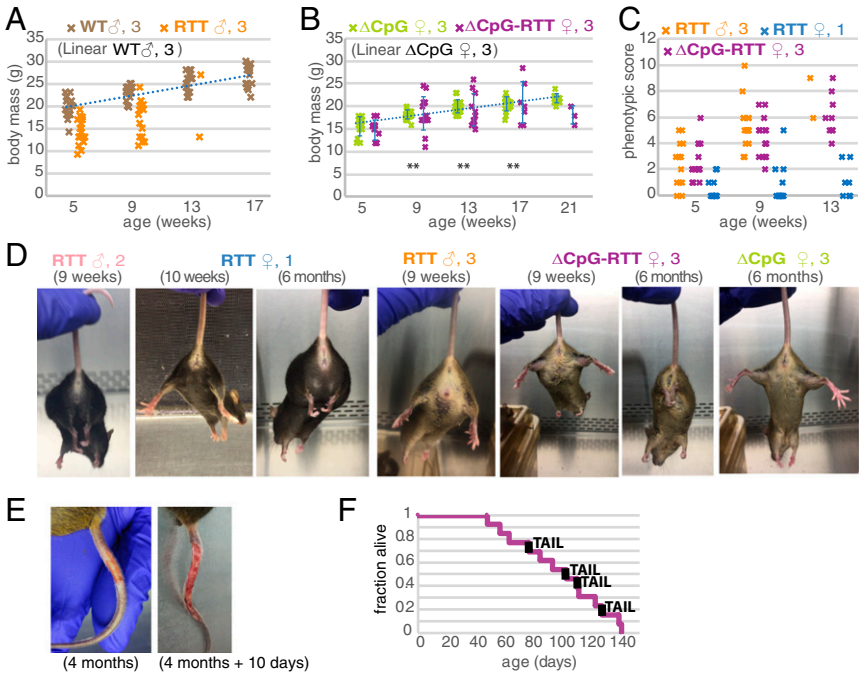

Fig. 5. Body mass and neurological phenotypes of ΔCpG-RTT females. (*A*) Mass in grams of WT and RTT male mice from cross 3 over time, with a linear trend line for the weight of the WT mice. (*B*) Mass in grams of WT and ΔCpG-RTT female mice from cross 3 over time, with a linear trend line for the weight of the WT mice. Error bars represent SDs. $^{**}P < 0.01$ for the SD between WT and ΔCpG-RTT. (*C*) Phenotypic scores of individual male RTT and female ΔCpG-RTT mice from cross 3 compared with RTT female mice from cross 1 over time. (*D*) Hindlimb clasping phenotype of indicated mice at noted ages. ΔCpG-RTT female did not exhibit hindlimb clasping at 9 wk. Control, ΔCpG female (*Right*). (*E*) Initial tail wound of an ΔCpG-RTT female at 4 mo (*Left*) and the expanded lesion at terminal stage occurring 10 d later (*Right*). (*F*) Kaplan–Maier curve for ΔCpG-RTT females from cross 3, with notation of mice that were euthanized for self-inflicted tail wounds.

clasping was typically the first distinctively observable symptom, before reduced movement and abnormal gait (Fig. 5*D*).

Finally, a most compelling neurological phenotype in the ΔCpG-RTT mouse model was repetitive behavior resulting in self-injury—a condition potentially similar to that described for human RTT girls. This manifested among others by obsessive self-grooming and biting of the tail. When under observation, WT mice typically self-groomed for only a few seconds in one sitting. In contrast, ΔCpG-RTT mice often groomed continuously for minutes at a time, sometimes extending beyond 10 min (Movies S10 and S11). When wounds occurred, they were initially confined to a small area but typically expanded over the course of days to a week to encompass nearly all of the tail (Fig. 5*E*). Over 30% of ΔCpG-RTT females were euthanized due to these severe injuries (Fig. 5*F*). Repetitive behavior and self-injury were not observed in any other RTT female model we tested, although others have reported such behavior in a mouse line with conditionally deleted *Mecp2* in GABAergic neurons (38). We also did not observe repetitive or self-injurious behaviors in diseased RTT males, nor in littermates carrying only the $Tsix^{\Delta CpG}$ mutation. Age could be a factor, as the incidence of injuries rose to >42% among ΔCpG-RTT females of >100 d old. Because male RTT mice generally perished before 100 d, they may not live long enough or be too severely affected to manifest repetitive and/or self-injurious behavior. Sexual dimorphism may be another factor (39, 40). Taken together, our study shows that the ΔCpG-RTT female mouse provides a good phenocopy of RTT disease for neurological and neuromotor phenotypes.

Discussion

By taking advantage of a modifier of X-chromosome inactivation, we have created a female RTT model with reduced cellular mosaicism, increased disease penetrance, and decreased disease variability. The ΔCpG-RTT female closely phenocopies the severe disease of the industry standard—the $Mecp2^{-/Y}$ male mice. In addition to manifesting neuromotor dysfunction, a failure to thrive, and an acutely shortened lifespan, the ΔCpG-RTT females also display a constellation of neurological symptoms. Strong tremors arise by weaning age and about a third of ΔCpG-RTT females mice develop repetitive behaviors such as obsessive grooming and self-biting, which result in injury and are potentially similar to those observed in human RTT girls, for whom hand wringing and self-biting can lead to self-injury. Because the ΔCpG-RTT mouse carries a dormant copy of *Mecp2* on the Xi, the mouse would indeed serve as an excellent model to test candidate Xi-reactivating drugs, of which a number has now been proposed (12–15, 17, 41), including a mixed-modality approach we developed recently (16). Furthermore, because the number of small animal models for repetitive and self-injurious behaviors is still limited and their pathophysiologies are poorly understood in general, the ΔCpG-RTT females may be an additional resource beyond their proposed utility for RTT research. Along with neurological, behavioral, and motor phenotypes, additional physiological tests for core RTT and related symptomatologies (22) would be of interest in the future.

A key finding to arise from our study of this improved female model is that even the presence of 5–10% MECP2 protein in the brain significantly extends life and lessens the severity of disease. MECP2 is thought to be cell autonomous, serving its function within the cells that produce it (42). The benefit of low-level expression for RTT could therefore in principle arise from either (*i*) a small number of cells expressing high-level MECP2, or (*ii*) a large number of cells expressing low-level MECP2. Both could improve fitness. Interestingly, the improved survival and phenotype of the *Mecp2-lox-stop-lox* male mice suggest that the latter possibility—a large number of cells expressing low-level MECP2 —ameliorates the RTT phenotype due to a "leaky" termination cassette that enables some 5–10% readthrough *Mecp2* transcription (8). Importantly, our immunostaining analysis of the brain suggests that the former possibility—a small number of cells expressing high-level MECP2—also improves fitness significantly (Fig. 3). This observation is consistent with the known role of *Tsix* in skewing XCI ratios and with the differences in skewing associated with the two alleles (ΔCpG and ΔF). A higher-than-expected level of MECP2 expression suggests positive selection in the brain. We also speculate that the rare $MECP2^{+}$ cells may confer a survival advantage of ~3 wk over the fully null males. As quantified by Western blot analysis of ΔCpG-RTT females, the level of MECP2 required to confer the additional survival benefit is <<5% of wild-type levels.

Intriguingly, our work shows a positive correlation between phenotypic improvement and MECP2 levels in the brain. This finding is consistent with the full spectrum of RTT disease phenotypes in affected humans, from severely affected boys with MECP2-null mutations, to strongly affected mosaic females with unfavorable XCI skewing, to the mildly affected females with more favorable XCI skewing (43). Significantly, in ΔCpG-RTT and ΔF-RTT mouse models, the positive correlation is nonlinear, with 5–10% increases extending life by five- to eightfold (Fig. 3*D*), further underscoring the disproportionate benefit. These findings are very welcome for the Xi-reactivation strategy, as it suggests that pharmaceutical mixtures need not boost MECP2 expression to the full extent for phenotypic impact.

Finally, as a general point for consideration, the cellular mosaicism caused by XCI—along with the estrous cycle—have long been offered as reasons for excluding females in research studies, resulting in the general practice of regarding male and female subjects as being equivalent (44). However, a recent metaanalysis of phenotypic data from 14,250 WT and 40,192 mutant mice found a large proportion of mammalian traits to be influenced by sex (45), with implications for interpretation of disease phenotypes. Studies of RTT and other X-linked disorders further accentuate the need for female models. The distinction of having an Xi and the more variable symptomatology are important reasons for inclusion of females in future RTT research.

Materials and Methods

Animal experiments were carried out in compliance with the Institutional Animal Care and Use Committee of Massachusetts General Hospital. Behavioral and molecular analyses were performed using standard procedures. A more detailed description and additional data are provided in *SI Appendix, Materials and Methods*.

ACKNOWLEDGMENTS. We thank all laboratory members for advice, protocols, and materials. L.L.G.C. was supported by the Belgian American Education Foundation, the Platform for Education and Talent and Research Foundation-Flanders for postdoctoral funding; R.J.K. by the Simons Foundation Research Initiative; and J.T.L. by National Institutes of Health Grant R01-DA36895 and the Rett Syndrome Research Trust and the International Rett Syndrome Foundation. J.T.L. is an investigator of the Howard Hughes Medical Institute.

1. Amir RE, et al. (1999) Rett syndrome is caused by mutations in X-linked MECP2, encoding methyl-CpG-binding protein 2. *Nat Genet* 23:185–188.
2. Lyst MJ, Bird A (2015) Rett syndrome: A complex disorder with simple roots. *Nat Rev Genet* 16:261–275.
3. Trappe R, et al. (2001) MECP2 mutations in sporadic cases of Rett syndrome are almost exclusively of paternal origin. *Am J Hum Genet* 68:1093–1101.
4. Chahrour M, Zoghbi HY (2007) The story of Rett syndrome: From clinic to neurobiology. *Neuron* 56:422–437.
5. Katz DM, et al. (2016) Rett syndrome: Crossing the threshold to clinical translation. *Trends Neurosci* 39:100–113.
6. Villard L (2007) MECP2 mutations in males. *J Med Genet* 44:417–423.
7. Giacometti E, Luikenhuis S, Beard C, Jaenisch R (2007) Partial rescue of MeCP2 deficiency by postnatal activation of MeCP2. *Proc Natl Acad Sci USA* 104:1931–1936.
8. Guy J, Gan J, Selfridge J, Cobb S, Bird A (2007) Reversal of neurological defects in a mouse model of Rett syndrome. *Science* 315:1143–1147.
9. Van Esch H, et al. (2005) Duplication of the MECP2 region is a frequent cause of severe mental retardation and progressive neurological symptoms in males. *Am J Hum Genet* 77:442–453.
10. Disteche CM (2012) Dosage compensation of the sex chromosomes. *Annu Rev Genet* 46:537–560.
11. Jégu T, Aeby E, Lee JT (2017) The X chromosome in space. *Nat Rev Genet* 18:377–389.
12. Bhatnagar S, et al. (2014) Genetic and pharmacological reactivation of the mammalian inactive X chromosome. *Proc Natl Acad Sci USA* 111:12591–12598.
13. Minajigi A, et al. (2015) Chromosomes. A comprehensive Xist interactome reveals cohesin repulsion and an RNA-directed chromosome conformation. *Science* 349: aab2276.
14. Minkovsky A, et al. (2015) A high-throughput screen of inactive X chromosome reactivation identifies the enhancement of DNA demethylation by 5-aza-2′-dC upon inhibition of ribonucleotide reductase. *Epigenetics Chromatin* 8:42.
15. Lessing D, et al. (2016) A high-throughput small molecule screen identifies synergism between DNA methylation and Aurora kinase pathways for X reactivation. *Proc Natl Acad Sci USA* 113:14366–14371.
16. Carrette LLG, et al. (2017) A mixed modality approach towards Xi reactivation for Rett syndrome and other X-linked disorders. *Proc Natl Acad Sci USA* 115:E668–E675.
17. Sripathy S, et al. (2017) Screen for reactivation of MeCP2 on the inactive X chromosome identifies the BMP/TGF-β superfamily as a regulator of XIST expression. *Proc Natl Acad Sci USA* 114:1619–1624.
18. Katz DM, et al. (2012) Preclinical research in Rett syndrome: Setting the foundation for translational success. *Dis Model Mech* 5:733–745.
19. Guy J, Hendrich B, Holmes M, Martin JE, Bird A (2001) A mouse Mecp2-null mutation causes neurological symptoms that mimic Rett syndrome. *Nat Genet* 27:322–326.
20. Chen RZ, Akbarian S, Tudor M, Jaenisch R (2001) Deficiency of methyl-CpG binding protein-2 in CNS neurons results in a Rett-like phenotype in mice. *Nat Genet* 27: 327–331.
21. Shahbazian M, et al. (2002) Mice with truncated MeCP2 recapitulate many Rett syndrome features and display hyperacetylation of histone H3. *Neuron* 35:243–254.
22. LeBlanc JJ, et al. (2015) Visual evoked potentials detect cortical processing deficits in Rett syndrome. *Ann Neurol* 78:775–786.
23. Krishnan K, Lau BY, Ewall G, Huang ZJ, Shea SD (2017) MECP2 regulates cortical plasticity underlying a learned behaviour in adult female mice. *Nat Commun* 8:14077.
24. De Filippis B, et al. (2015) Deficient purposeful use of forepaws in female mice modelling Rett syndrome. *Neural Plast* 2015:326184.
25. Samaco RC, et al. (2013) Female Mecp2(+/–) mice display robust behavioral deficits on two different genetic backgrounds providing a framework for pre-clinical studies. *Hum Mol Genet* 22:96–109.
26. Johnson CM, Cui N, Zhong W, Oginsky MF, Jiang C (2015) Breathing abnormalities in a female mouse model of Rett syndrome. *J Physiol Sci* 65:451–459.
27. Cobolli Gigli C, et al. (2016) MeCP2 related studies benefit from the use of CD1 as genetic background. *PLoS One* 11:e0153473.
28. Vogel Ciernia A, et al. (2017) Early motor phenotype detection in a female mouse model of Rett syndrome is improved by cross-fostering. *Hum Mol Genet* 26: 1839–1854.
29. Brown CJ, et al. (1992) The human XIST gene: Analysis of a 17 kb inactive X-specific RNA that contains conserved repeats and is highly localized within the nucleus. *Cell* 71:527–542.
30. Lee JT, Davidow LS, Warshawsky D (1999) Tsix, a gene antisense to Xist at the X-inactivation centre. *Nat Genet* 21:400–404.
31. Lee JT (2000) Disruption of imprinted X inactivation by parent-of-origin effects at Tsix. *Cell* 103:17–27.
32. Lee JT (2002) Homozygous Tsix mutant mice reveal a sex-ratio distortion and revert to random X-inactivation. *Nat Genet* 32:195–200.
33. Knudsen GP, et al. (2006) Increased skewing of X chromosome inactivation in Rett syndrome patients and their mothers. *Eur J Hum Genet* 14:1189–1194.
34. Lee JT, Lu N (1999) Targeted mutagenesis of Tsix leads to nonrandom X inactivation. *Cell* 99:47–57.
35. Goffin D, Zhou ZJ (2012) The neural circuit basis of Rett syndrome. *Front Biol (Beijing)* 7:428–435.
36. Jones BJ, Roberts DJ (1968) The quantiative measurement of motor inco-ordination in naive mice using an acelerating rotarod. *J Pharm Pharmacol* 20:302–304.
37. Tesla R, et al. (2012) Neuroprotective efficacy of aminopropyl carbazoles in a mouse model of amyotrophic lateral sclerosis. *Proc Natl Acad Sci USA* 109:17016–17021.
38. Chao HT, et al. (2010) Dysfunction in GABA signalling mediates autism-like stereotypies and Rett syndrome phenotypes. *Nature* 468:263–269.
39. Labad J, et al. (2005) Female reproductive cycle and obsessive-compulsive disorder. *J Clin Psychiatry* 66:428–435, quiz 546.
40. Claes L, Vandereycken W, Vertommen H (2007) Self-injury in female versus male psychiatric patients: A comparison of characteristics, psychopathology and aggression regulation. *Pers Individ Dif* 42:611–621.
41. Chan KM, Zhang H, Malureanu L, van Deursen J, Zhang Z (2011) Diverse factors are involved in maintaining X chromosome inactivation. *Proc Natl Acad Sci USA* 108: 16699–16704.
42. Kishi N, Macklis JD (2010) MeCP2 functions largely cell-autonomously, but also non-cell-autonomously, in neuronal maturation and dendritic arborization of cortical pyramidal neurons. *Exp Neurol* 222:51–58.
43. Huppke P, et al. (2006) Very mild cases of Rett syndrome with skewed X inactivation. *J Med Genet* 43:814–816.
44. Prendergast BJ, Onishi KG, Zucker I (2014) Female mice liberated for inclusion in neuroscience and biomedical research. *Neurosci Biobehav Rev* 40:1–5.
45. Karp NA, et al.; International Mouse Phenotyping Consortium (2017) Prevalence of sexual dimorphism in mammalian phenotypic traits. *Nat Commun* 8:15475.